A Thesis for the Degree of Master of Science

Metabolomic Analysis of *Vibrio vulnificus* Biofilm and Validation of Control Target

패혈증 비브리오균 바이오필름의 대사체적 분석과 바이오필름 제어 타겟의 확인

February, 2015

Wonleoung Lee

Department of Agricultural Biotechnology
College of Agriculture and Life Sciences
Seoul National University

석사학위논문

Metabolomic Analysis of *Vibrio vulnificus* Biofilm and Validation of Control Target

지도교수 최 상 호

이 논문을 석사학위논문으로 제출함

2015 년 2 월

서울대학교 대학원

농생명공학부

이 원 령

이원령의 석사학위논문을 인준함

2015 년 2 월

위원장 장 판 식 (인)

부위원장 최 상 호 (인)

위원 강 동 현 (인)

Abstract

Biofilms are assemblages of microbial cells enclosed in self-produced extracellular polymeric matrix (EPM). Biofilm formation provides *Vibrio vulnificus* with resistances to antimicrobial agents and a variety of stresses in the environment. In order to gain insight into the cellular mechanisms in mature biofilms, the global metabolite profiling of *V. vulnificus* biofilms and planktonic cells was analyzed by using gas chromatography-time of flight mass spectrometry (GC-TOF-MS) and multivariate statistical analysis. Principal component analysis (PCA) and partial least-squares discriminant analysis (PLS-DA) showed significant differences in metabolic profiles between biofilms and planktonic cells. The levels of some amino acids, monosaccharides and nucleotides were elevated in biofilms compared to the planktonic counterparts. These metabolites appear to function as building blocks for structural components of extracellular matrix. Metabolites involved in the anaerobic energy production, such as glycolysis and pyruvate fermentation, were increased in biofilms. These suggest that *V. vulnificus* may obtain energy by using glycolysis and pyruvate fermentation in biofilms. The amounts of product of putrescine biosynthetic pathway in bioflms were also greater than in the planktonic cells. These results suggested that putrescine may have a positive effect on formation of *V. vulnificus* biofilms. Furthermore, the amounts and expression levels of the metabolites and genes, respectively, involved in *N*-acetylglucosamine (GlcNAc) utilization were highly increased in *V. vulnificus* biofilms. The combined results

suggest that, when *V. vulnificus* forms mature biofilms and encounters conditions of low-nutrient, GlcNAc-specific phosphotransferase system (PTS) may transfer GlcNAc which is derived from extracellular environments. To find out whether GlcNAc-specific PTS affects biofilm forming ability of *V. vulnificus,* biofilm forming activities of the wild type and GlcNAc-specific phosphotransferase (*ptsG*) mutant were compared. Under the condition of low carbon source, biofilm forming activity was reduced in the *ptsG* mutant compared to the wild type and recovered in the complemented strain. Composition analysis of exopolysaccharide (EPS) using GC-TOF-MS revealed that GlcNAc is one of the constituent of EPS. In these aspects, when bacterial cells in *V. vulnificus* biofilms are faced with adverse conditions, such as insufficient nutrient, PtsG appears to transport GlcNAc, as a carbon source, which stems from extracellular matrix. Consequently, *V. vulnificus* in biofilms exhibits a distinct mode of growth characterized by matrix components syntheses, anaerobic energy production, polyamine metabolism and *N*-acetylglucosamine utilization.

Key words: *Vibrio vulnificus*, Biofilm, Metabolomics, *N*-acetylglucosamine, *ptsG*

Student Number: 2013-21183

Contents

List of Figures

List of Tables

I. INTRODUCTION

Vibrio vulnificus, a Gram-negative, motile, curved and rod-shaped bacterium, is the causative agent of food-borne disease including gastroenteritis and life-threatening septicemia (Jones & Oliver, 2009). Biofilms can be defined as communities of microorganisms that are attached to a surface (O'Toole, G *et al.,* 2000). Like many other pathogenic bacteria, *V. vulnificus* forms biofilms in natural ecosystems. Bacterial biofilm cells are highly resistant to various stresses, such as antibiotics and host immune defense systems, relative to planktonic counterparts. Biofilms of pathogenic bacteria are considered one of the most important factors of outbreaks and account for 65% of bacterial infections in humans (Costerton, 2001). Also, biofilms have been considered a significant factor in food hygiene since biofilms may contain pathogenic bacteria which increases post-processing contamination and risk to public health (Shi & Zhu, 2009).

In biofilms, cells grow in multicellular aggregates that are encased in an extracellular polymeric matrix (EPM) produced by the bacteria themselves (Branda *et al.,* 2005; Hall-Stoodley & Stoodley 2009). EPM, which forms the scaffold for the three-dimensional architecture of the biofilms, plays a role as adhesion to surfaces and cohesion in the biofilms (Flemming *et al.,* 2010). Many studies about control of biofilm formation have been conducted by several techniques including transposon mutagenesis, transcriptomics and proteomics. Transposon mutagenesis

and other genetic screens were allowed the identification of genes involved in biofilm formation in *Escherichia coli* K-12 (Genevaux *et al.,* 1996) and the confirmation of the importance of matrix-synthesis pathways in *Pseudomonas aeruginosa* and *E. coli* K-12 (Boyd *et al.,* 1995; Danese *et al.,* 2000; Davies *et al.,* 1993). In *Pseudomonas putida* biofilms, proteomic analysis and substrative cDNA libraries showed that protein patterns changed soon after the initial adhesion on the surface (Sauer *et al.,* 2001). Proteome and transcriptome analysis were used for the global approaches of *P. aeruginosa* biofilms (Whiteley *et al.,* 2001).

Metabolomics is an effective approach that can describe an organism's phenotype, at cellular, tissue or whole organism level (Lin *et al.,* 2006). Metabolism represents one of the most dynamic aspects of cellular physiology and by studying it, one can obtain a snapshot of underlying physiological processes (Fiehn, 2002). Thus, metabolomics has wide applicability to a number of areas including medicine, plant sciences, toxicology and food sciences. In these aspects, metabolomics is a powerful tool for complementing other 'omics' studies. Especially, in *Vibrio* spp., this is one of the first studies to perform a global metabolite profiling of both biofilms and planktonic cells using metabolomics technique.

In this study, the global metabolite profiling of *V. vulnificus* biofilms and planktonic cells was analyzed by using GC-TOF-MS. As a result, I found out several biofilm-specific physiological pathways. Based on the metabolome and transcriptome data of *V. vulnificus* biofilms, I selected a target gene related to GlcNAc-specific PTS

(PtsG). This study suggested that GC MS-based metabolomic approach can be used to gain insight into the control of biofilm formation.

II. MATERIALS AND METHODS

Culture conditions and biofilm formation. The strain used in this study is listed in Table 1. *V. vulnificus* MO6-24/O was grown in Luria-Bertani (LB) medium supplemented with 2.0% (wt/vol) NaCl (LBS) at 30°C to prepare an overnight culture. The *Vibrio fisheri* minimal medium containing 32.6 mM glycerol (VFMG) was used for biofilm formation (Kim *et al*., 2013). An aliquot of cultures (480 μl) grown to an A_{600} of 0.8 with LBS broth was used to inoculate 8 ml of VFMG in a 6-well culture plate (SPL, Seoul, South Korea). Biofilms were formed by incubating these cultures at 30°C without shaking. Biofilms and planktonic cells were sampled at peak time point (6hours after incubation). Planktonic cells from the wells were collected by pipetting and harvested by centrifugation at 5,000 × g for 7 min at 4 ^{o}C and washed with cold phosphate-buffered saline (PBS; pH 7.4). Biofilm cells were collected with a cell scraper (SPL) and washed with cold PBS. Washed cell pellets were kept at -80°C until extraction. All samples were prepared in biological duplicates. To confirm the stages of biofilm development, biofilms were quantitated using crystal violet staining at every hour (Kim *et al*., 2013). Biofilms were formed by standing the 6-well culture plates (SPL) containing 8 ml culture with VFMG at 30^{o}C. Once the planktonic cells were removed, the biofilm cells on the wall were washed with PBS, and then stained with 1% (wt/vol) crystal violet (CV) solution for 15 minutes at room temperature. Biofilms were quantitated by measuring the amount of CV eluted from the biofilms as an absorbance at 570 nm (A_{570}) (Kim *et*

al., 2009).

Metabolites extraction. For biofilm intracellular metabolite extraction, cells were sonicated (Bioruptor, Tokyo, Japan) with 1 ml of extraction solvent, mixture of acetonitrile / methanol / water (Gibco, NY, US) (AMW; 2:2:1, v/v/v) at 4°C for 30 minutes (Shin *et al.*, 2010a). After sonication, samples were cetrifuged at maximum speed for 20 minutes at 4°C. The supernatant was transferred to the new tube. Samples were normalized to the protein concentration by bradford assay prior to derivatization of metabolites. After normalization, samples were transferred to the eppendorf tube and concentrated to dryness in a vacuum concentrator (Biotron, Seoul, Korea) for 5 hours. Dried bacterial pellets were kept at -80°C until next step.

Derivatization of metabolites. Prior to GC-TOF-MS analysis, dried metabolites were derivatized by methoxyamination and silylation. Briefly, 50 μl of 20 mg/ml methoxyamine hydrochloride in pyridine was added to metabolite samples and incubated for 90 minutes at 30°C in the thermo mixer (Eppendorf, Hamburg, Germany) with 600rpm. The metabolites samples were then mixed with 50 μL of *N*-methyl-*N*-trimethylsilyltrifluoroacetamide (MSTFA) and incubated for 30 minutes at 37°C with 600rpm (Kim *et al*., 2013a). After derivatization, samples were cetrifuged at 16000 × g for 2 minutes at room temperature. The upper layer was transferred to GC vial.

GC-TOF-MS analysis. The derivatized metabolite samples were analyzed by GC-TOF-MS using an Agilent 7890A gas chromatography (Agilent Technologies, Wilmington, DE) coupled with a Pegasus III TOF MS (LECO, St. Joseph, MI). Each sample (1 µl) was injected by an autosampler (Agilent 7693) equipped with a Rtx-5MS capillary column (30 m length × 0.25 mm i.d. × 0.25 µM film thickness-Agilent J&W GC column) in splitless mode. Helium was used as the carrier gas at a constant flow rate of 1.5 ml/minutes. The injector temperature was 250°C, and the injection volume was 1 µl. The oven temperature program commenced from 75°C for 2 minutes, followed by 300°C from 2 to 15 minutes, with a 15°C/minute hold, and finally a hold of 3 minutes, with a transfer line temperature of 240°C.

In MS, ionization was at − 70 V (electron energy) with a source temperature of 230°C. The detector voltage was 1450 V, and the mass range was set at 45–800 m/z with an acquisition rate of 10 spectra per second.

Data processing. GC-TOF-MS raw data files were converted to computable document format (*.cdf) by the inbuilt data processing software of the Agilent GC system programs. After obtaining the CDF format, the files were subjected to preprocessing, peak extraction, retention time correction and alignment using metAlign software package (http://www.metalign.nl). After analysis, the resulting peak list was obtained as a .txt file, which was later exported to Microsoft Excel (Microsoft, Redmond, WA, USA). The Excel file contained the corrected peak

retention time, peak area and corresponding mass (m/z) data matrix for further analysis.

Statistical analysis. SIMCA-P software 12.0 (Umetrics, Umeå, Sweden) was used for principle component analysis (PCA). Partial least-squares discriminate analysis (PLS-DA) was carried out using auto-scaled and log-transformed data to identify the metabolites showed variation between biofilm and planktonic samples. Based on the variable importance in projection (VIP) values (> 0.7) and a threshold of < 0.05 for Student's t-test of individual samples, the variable selection was made by STATISTICA 7.0 and compared by box-and-whisker plots using SigmaPlot 10.0. Annotation of peaks were based on standard retention times, m/z, and existing references.

Generation of the *V. vulnificus ptsG* mutant. The *ptsG* gene on chromosome was amplified and inactivated *in vitro* by deletion of the most of *ptsG* ORF using the PCR-mediated linker-scanning mutation method as described elsewhere (Lee *et al.*, 2007). Briefly, pairs of primers PtsG_F1-F and PtsG_F1-R (for amplification of the 5' amplicon) or PtsG_F2-F and PtsG_F2-R (for amplification of the 3' amplicon) were designed and used as listed in Table 2. The Δ *ptsG*, a 756 bp deleted *ptsG*, was amplified by PCR using the mixture of both amplicons as the template and PtsG_F1-F and PtsG_F2-R as primers. The resulting Δ *ptsG* was ligated with SalI-SphI digested pDM4 (Milton *et al.,* 1996) to form pWL1410 (Table 1). In order to

generate the *ptsG* mutant WL148 by homologous recombination, *E. coli* S 17-1 λ *pir, tra* containing pWL1410 was used as a conjugal donor in coujugation with *V. vulnificus* MO6-24/O as indicated in Table 1. All of the conjugation and isolation of the transconjugants were conducted using the methods previously described (Oh *et al*., 2009).

Genetic complementation of *ptsG* null mutant. Complementation was carried out by introduction of the *ptsG* ORF under P_{BAD} promoter control of pJK1113. The *ptsG* ORF was PCR-amplified from *V. vulnificus* MO6-24/O genomic DNA using a pair of primers PtsG_Comp_F and PtsG_Comp_R. The amplified *ptsG* DNA fragment was digested with SalI and and then cloned into predigested pJK1113 at SalI and NcoI, sites. The resultant plasmid, pWL1412 had been transformed to *E. coli* S 17-1 λ *pir, tra* and selected by growth on kanamycin (100 μg/ml). Selected *E. coli* was used as conjugal donor to Δ *ptsG*. Also, E.coli S 17-1 λ pir, tra harboring pJK1113 was transformed into wild type Δ *ptsG* for control. Conjugation was conducted and the transcoujugants were used for subsequent biofilm assays. Abilities to form biofilms of complemented strain and control strains were determined using the crystal violet staining assay, previously described. Bacterial strains were grown at 30℃ for 24 hours with 0.002% arabinose and 100 μg/ml kanamycin. Modified VFMG (containing 10, 1, 0.1mM glycerol) was used for biofilm formation. Following procedures were performed as described above.

Extraction and analysis of exopolysaccharide (EPS). EPS was extracted by a modified method as described elsewhere (Enos-Berlage *et al.,* 2000). Briefly, were grown on LBS agar plates for 20 hours at 30℃, forming bacterial lawn. Bacteria were scraped from the plates and suspended in the 5 ml of PBS, adjusting the OD600 1.0 for the same bacterial biomass in each resuspension. Samples were vigorously vortexed for 1 minute and shaken at 200 rpm for 40 minutes at 30℃ to elute loosely associated extracellular matrix. Vortexing and shaking were repeated twice. After cells and debris were removed by centrifugation at 10000 × g for 15 minutes, supernatants were treated with RNaseA (50 mg/ ml, Sigma) and Nuclease (50 mg/ ml, Novagen) in the presence of 10 mM $MgCl_2$ at 37℃ for 12 hours. After 12 hours, proteinase K (200 mg/ ml) was added to the reaction mixtures and incubated at 37℃ for 17 hours. Subsequently, the remained polysaccharide fractions were extracted twice with phenol-chloroform, and precipitated with 2.5 x volumes of 100% ethanol and NaOAC (final concentration 0.3 M). The samples were stored at deep freezer during overnight. The samples were centrifuged at 4℃, for 1 hour at maximum speed and then, supernatants were removed. Samples were washed with 70% ethanol and dried in the air. Dried pellets were hydrolyzed with 400 μl of 2 M trifluoroacetic acid (TFA) at 100℃ for 4 hours (Kim *et al.,* 2011). Then, all samples were dried down in a vacuum concentrator for 1.5 hours. Dried pellets were derivatized and analyzed by GC-TOF-MS. All procedures were the same as those of described above.

Table 1. Bacterial strains and plasmids used in this study.

Strain or plasmid	Relevant characteristics [a]	Reference or source
Bacterial strains		
V. vulnificus		
MO6-24/O	wild type *V. vulnificus,* virulent	Laboratory collection
WL147	MO6-24/O with Δ *ptsG*	This study
E. coli		
DH5a	*supE44 DlacU169 (f80 lacZ D*M15*) hsdR17 recA1 endA1 gyrA96 relA1 relA1 thi-1 relA1*; plasmid replication	Laboratory collection
S 17-1λ*pir*	cojugal donor; Sm^r; host for π-requiring plasmids	Laboratory collection
Plasmid		
pGEM-T easy	PCR product cloning vector;Ap^r	Promega
pDM4	suicide vector; *ori* R6K; Cm^r	Milton *et al.,* 1996
pWL1410	pDM4 with Δ *ptsG*; Cm^r	This study
pJK1113	pBAD24; oriT; nptI; Ap^r, Km^r	Laboratory collection
pWL1412	pJK1113 with *ptsG*	This study

[a] Ap^r, ampicillin resistant; Km^r, kanamycin resistant; Cm^r, chloramphenicol resistant; Sm^r, streptomycin resistant.

Table 2. Oligonucleotides used in this study.

Name	Oligonucleotide sequence, 5' → 3'	Use
PtsG_F1-F	TGC GGC GCT CTT ACT ACG TTT G	Mutant construction
PtsG_F1_R	GAA GGA TCC AAT AGG CAC TAG ACG TTT G	Mutant construction
PtsG_F2_F	ATT GGA TCC TTC GTA CTG CTA CTA ATC G	Mutant construction
PtsG_F2_R	CTT CTG ATA GGT CTT CGT TGA CAC CG	Mutant construction
PtsG_Comp_F	ATC CAT GGT TAT GCT ACC TAT CGC AAC	Vector for genetic complementation
PtsG_Comp_R	ATG TCG ACC TTT TCA TAT CAT TCA GAG TG	Vector for genetic complementation

III. RESULTS

Biofilm formation in the glycerol containing minimal media.

V. vulnificus MO6-24/O formed biofilms in the 6-well culture plates (Fig. 1). There are three stages of biofilm development: (i) initial attachment, (ii) maturation, (iii) dispersion. As biofilms age, the amount of biofilms reached the peak point at 6 hours after incubation. Then, biofilms dramatically reduced from the peak point. To characterize mechanisms of mature biofilms, biofilms and planktonic cells were collected at the peak time point.

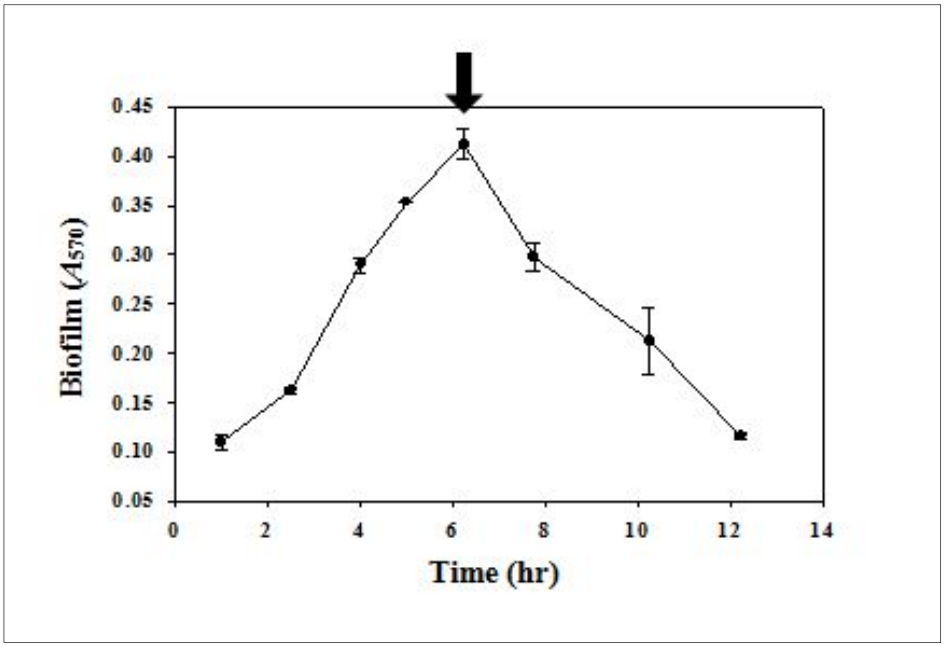

Fig. 1. Biofilm formation of *V. vulnificus* MO6-24/O. The wild type biofilms were grown on the 6-well culture plate wells containing VFMG and quantitated using crystal violet staining. The arrow indicates the time point for collecting biofilms and planktonic cells. Error bars represent the SEM.

Schematic work flow of metabolomics study.

GC-TOF-MS is highly sensitive with semi-automated metabolite identification capabilities. Thus, it is frequently used for metabolomics study. To detect the major primary metabolite in *V. vulnificus* biofilms and planktonic cells, GC-TOF-MS was selected for this metabolomic analysis. Metabolome sampling is one of the most important factors that determine the quality of metabolomics data (Kim *et al*., 2013a). It is essential that the sample reflects the biological status of the cell. Thus, sampling procedures were conducted rapidly.

The crucial steps in sample preparation are quenching and metabolite extraction. For growing microorganisms, the turnover rates of metabolites are extremely fast. Thus, to generate an authentic profile of a system's metabolic composition cellular metabolism should first be quenched (Marcinowska *et al*., 2011). The most widely used quenching method is to add cold methanol, prior to collecting cells by centrifugation (Sellick *et al*., 2009). However, when cold methanol quenching was applied, serious losses of intracellular metabolites due to cell leakage were observed in bacteria. As an alternative to cold methanol quenching, the fast filtration method was developed to be effective in minimizing the losses of intracellular metabolites both in Gram-negative and Gram-positive bacteria (Shin *et al*., 2010).

Following quenching the metabolites are extracted using methods that lyse the cell. Cell breakage methods can be chemical or mechanical, the latter involving application of pressure and/or shearing forces of some kind. (Marcinowska *et al*., 2011). The effects of different extraction solvents have revealed. In gram negative

bacteria, a mixture of acetonitrile/ methanol/ water (AMW; 2:2:1) showed the enhancement of the extraction efficiency (Shin *et al*., 2010). Finally, metabolites were derivatized by methoxyamination and silylation. In order to make compounds volatile and accessible for analysis by GC-MS, chemical modification of the polar functional groups using derivatization reagents is necessary.

V. vulnificus MO6-24/O biofilm and planktonic cells were grown on the 6-well culture plate

Extraction with 4 °C AMW Sonicator, 35min.

Freeze drying 8hours

Derivertization of dried metabolites Oximation and Silylation

GC-TOF-MS

File conversion to Net CDF files
Data processing with 'Metalign'

Multivariate analysis

Metabolites identification using standards and libraries

Fig. 2. Schematic flow of total experimental processes. After sample preparation, the metabolites were extracted in AMW at 4°C by sonicator. Extracted metabolites were concentrated to dryness; following dried metabolites were derivatized by methoxyamination and silylation. The derivatized metabolite samples were analyzed by GC-TOF-MS. GC-TOF-MS raw data files were converted to computable document format (*.cdf) by the inbuilt data processing software of the Agilent GC system programs. After obtaining the CDF format, the files were subjected to preprocessing, peak extraction, retention time correction and alignment using metAlign software package (http://www.metalign.nl). SIMCA-P software 12.0 (Umetrics, Umeå, Sweden) was used for principle component analysis (PCA). Partial least-squares discriminate analysis (PLS-DA) was carried out using auto-scaled and log-transformed data to identify the metabolites showed variation between biofilm and planktonic samples.

Multivariate statistical analysis of biofilms and plnktonic cells.

Principal component analysis (PCA) was used to identify significant differences in the data. PCA is an unsupervised statistical modeling technique that separates samples based on their differences from each other, whereas Partial least-squares discriminant analysis (PLS-DA) is supervised, allowing for the definition of classes before the test is performed.

All samples were prepared in biological duplicates and analytical duplicates. (Fig. 3). PCA and PLS-DA showed significant differences in metabolic profiles between biofilms and planktonic cells. The first Principal Component (PC), which accounts for 35.9% of the variability in the data, separates the biofilms from the planktonic samples. The second PC, which describes an additional 20.6% of the variability, isolates the biofilms from the planktonic samples (Fig. 3A). The first Partial Least Squares (PLS), which accounts for 35.0% of the variability in the data, separates the biofilms from the planktonic samples. The second PLS, which describes an additional 21.3% of the variability, isolates the biofilms from the planktonic samples (Fig. 3B).

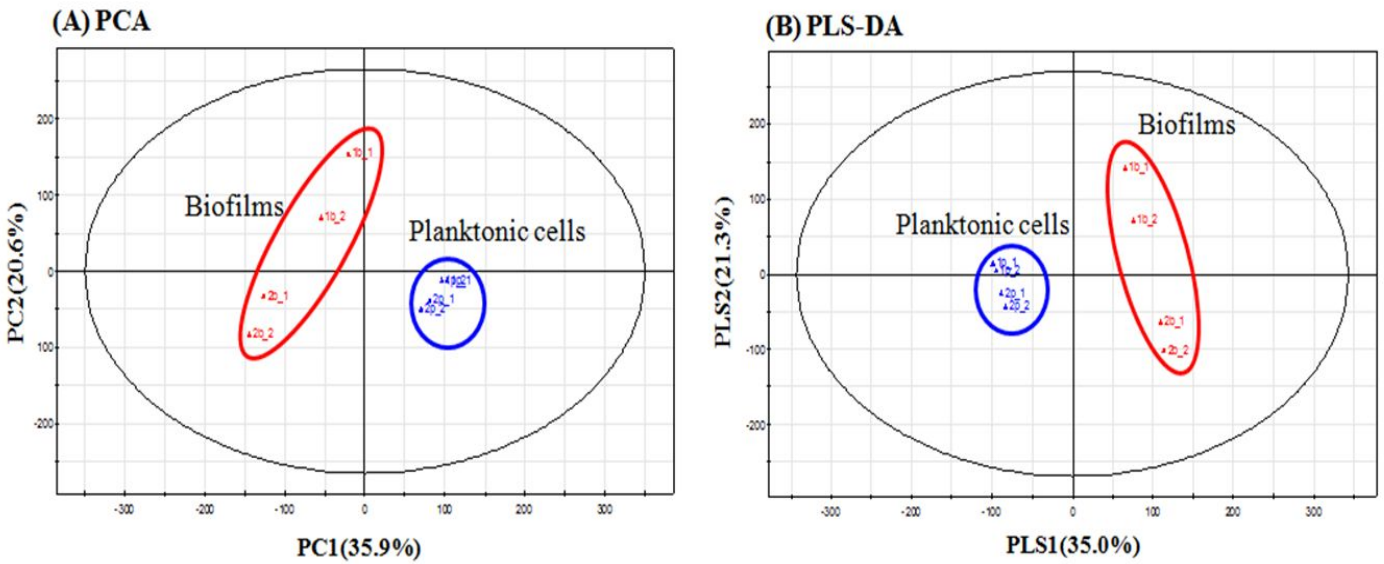

Fig. 3. PCA(A) and PLS-DA(B) score plot for *V. vulnificus* MO6-24/O biofilms and planktonic samples. These plots explained that the metabolism of *V. vulnificus* biofilms is different from that of planktonic cells. PCA, Principal Component Analysis; PLS-DA, Partial Least Squares-Discriminant Analysis; Red circle, biofilms; Blue circle, planktonic cells.

Identification of metabolites from standards and libraries.

The metabolites reflecting variation between the *V.vulnificus* biofilms and planktonic cells were identified based on the VIP (variable importance of the projection) and *p*-value. Identification of metabolites was based on their retention time in comparison with standards and in-house libraries (Table 3). A total of 53 primary metabolites, including 10 organic acids, 18 amino acids, 12 sugars and sugar alcohols, 13 extra metabolites showed significant variation among the samples (Fig. 4). The levels of 38 metabolites, such as some amino acids, monosaccharides and nucleotides were elevated in biofilms compared to the planktonic counterparts. In planktonic cells, 15 metabolites were higher than biofilms.

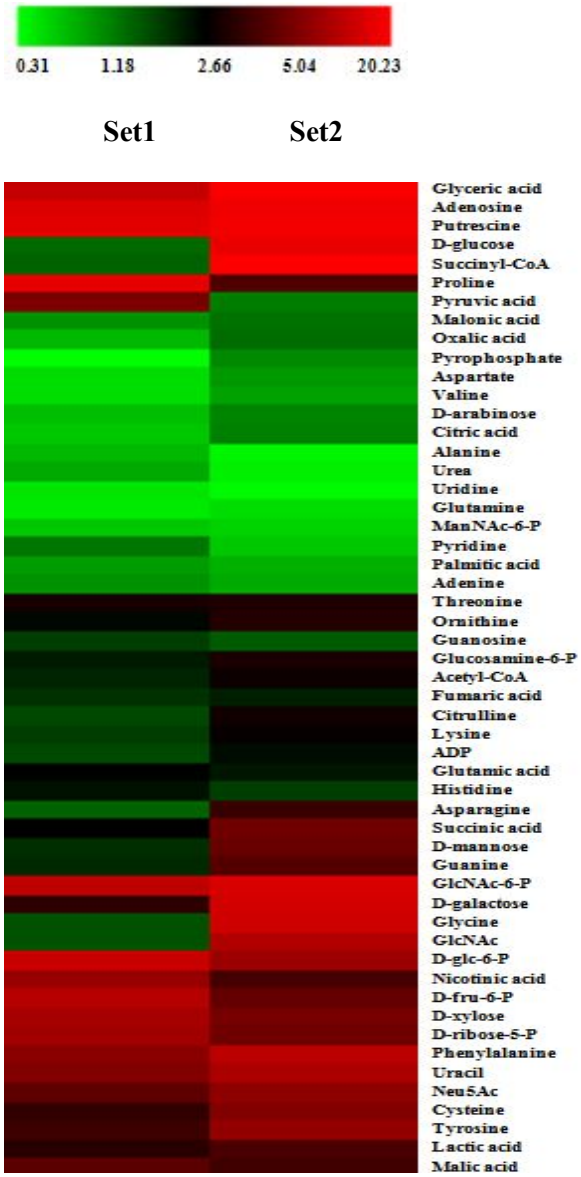

Fig. 4. Clustered heat map of metabolomic analysis. Significantly different metabolites between *V. vulnificus* biofilms and planktonic cells during mature stage. The number stands for the fold change ratio of biofilms : planktonic cells (Variable selection: VIP value >0.7 and *p*-value <0.05). Set1, Set2; biological duplicates.

Table 3. The most significantly different metabolites identified in the *V. vulnificus* biofilms relative to the planktonic couterparts.

[a]Compound	[b]RT(min)	[c]MS Fragmentation(m/z)	[d]ID	[e]Fold change
Amino acids				
Glycine	**7.39**	**45,73,86,117,147,174,248,276,357**	**MS/STD**	**3.25**
Proline	**7.30**	**45,59,73,84,100,133,142,216**	**MS/STD**	**8.14**
Threonine	**8.13**	**45,73,86,117,147,219,248,291,350**	**MS/STD**	**2.81**
Phenylalanine	**10.13**	**45,73,100,147,192,218,266**	**MS/STD**	**5.12**
Ornithine	**11.54**	**73,142,200,258,330**	**MS/STD**	**2.94**
Lysine	**12.21**	**45,59,73,82,100,132,147,154,166,218,238**	**MS/STD**	**2.13**
Cysteine	**9.58**	**59,73,91,100,116,132,147,163,204,220,294**	**MS/STD**	**4.13**
Glutamic acid	**10.06**	**45,73,100,128,174,204,246,274,320**	**MS/STD**	**2.34**
Histidine	**6.77**	**45,59,73,82,100,132,147,154,166,218,238,254**	**MS/STD**	**2.05**
Asparagine	**10.46**	**45,59,73,100,116,147,188,231,259**	**MS/STD**	**2.48**
Tyrosine	**12.36**	**45,73,100,147,179,218,249,280,354,382**	**MS/STD**	**4.34**

Table 3. The most significantly different metabolites identified in the *V. vulnificus* biofilms relative to the planktonic couterparts (continued).

[a]Compound	[b]RT(min)	[c]MS Fragmentation(m/z)	[d]ID	[e]Fold change
Sugars and Sugar alcohols				
D-galactose	**12.16**	**45,73,103,117,129,147,160,189,205,217,319**	**MS/STD**	**5.80**
D-mannose	**12.20**	**45,59,73,89,103,117,129,147,160,189,205,217, 319**	**MS/STD**	**3.25**
GlcNAc	**13.57**	**59,73,89,116,147,191,217,245**	**MS/STD**	**4.02**
D-fru-6-P	**14.71**	**59,73,103,147,191,217,315,357,387**	**MS/STD**	**5.63**
D-glc-6-P	**14.79**	**59,73,101,147,191,217,247,299,357,387**	**MS/STD**	**6.49**
Glucosamine-6-P	**15.07**	**73,101,147,159,217,299,387**	**MS/STD**	**2.52**
Neu5Ac	**16.46**	**45,59,73,89,103,117,133,147,205,217,246**	**MS/STD**	**4.72**
D-xylose	**10.41**	**45,59,73,89,103,117,133,147,160,189,205,217, 307**	**MS/STD**	**5.32**
GlcNAc-6-P	**15.70**	**45,59,73,87,101,129,147,211,243,299,315,357, 387**	**MS/STD**	**7.91**
D-glucose	**12.18**	**59,73,103,147,189,205,319**	**MS/STD**	**7.29**

Table 3. The most significantly different metabolites identified in the *V. vulnificus* biofilms relative to the planktonic couterparts (continued).

[a]Compound	[b]RT(min)	[c]MS Fragmentation(m/z)	[d]ID	[e]Fold change
Oranic acid				
Lactic acid	**4.92**	**63,79,81,91,92,106**	**MS**	**3.51**
Nicotinic acid	**7.25**	**51,78,90,106,117,136,180,195**	**MS/STD**	**4.67**
Succinic acid	**7.41**	**45,55,73,86,129,147,172,218,247**	**MS/STD**	**3.52**
Fumaric acid	**7.70**	**45,53,59,69,73,83,99,115,133,143,147,217,245**	**MS/STD**	**2.05**
Malic acid	**8.99**	**45,53,59,69,73,83,99,115,133,143,147,217,245**	**MS/STD**	**3.88**
Glyceric acid	**11.43**	**56,72,73,157,197,256,279,298**	**MS**	**13.63**
Pyruvic acid	**12.38**	**45,73,103,130,158,190,217,247**	**MS/STD**	**2.89**

Table 3. The most significantly different metabolites identified in the *V. vulnificus* biofilms relative to the planktonic couterparts (continued).

[a]Compound	[b]RT(min)	[c]MS Fragmentation(m/z)	[d]ID	[e]Fold change
etc				
ADP	7.13	59,73,89,103,133,147,7193,211,299,314	MS/STD	2.04
Uracil	7.68	45,73, 85, 99,113,147,169,241	MS/STD	5.56
D-ribose-5-P	13.45	59,73,75,77,89,101,103,131,211,217,299,301, 315,316	MS	5.24
Guanine	13.62	59,73,99,147,238,264,294,352	MS/STD	3.09
Adenosine	16.37	45,59,73,84,103,129,147,165,192,217,236,259, 280	MS/STD	12.61
Guanosine	17.03	45,73,103,147,189,217,245,280,324,368	MS	3.09
Acetyl-CoA	13.96	52,74,78,80,88,89,107,137,166,167,183,201	MS	2.32
Putresine	10.90	55,56,57,61,70,72,85,97,99,114,130,132,146, 161,187, 201, 361	MS	14.99
Succinyl-CoA	7.40	112,126,146,179,224,253,265,309,312,328,344, 432,433	MS	10.88

[a]Identified metabolites depended on variable importance projection (VIP) value under 0.7 and p-value <0.05.

[b]Retention time.

[c]m/z values are the selected ions for identification and quantification of individual derivatized metabolies.

[d]Identification: MS, mass spectrum was consistent with those of nist and in-house libraries; STD, mass spectrum was consistent with that of standard compound.

[e]Fold change ratio of biofilms : planktonic cells.

Carbohydrate metabolism pathway analysis.

The metabolic pathways in Figure 5 show that carbohydrate utilization related metabolites were higher in biofilms than planktonic cells. The levels of glucose, mannose, fructose, glycerate, fructose-6-p, glucose-6-p, glucosamine-6-p, pyruvate and *N*-acetylglucosamine, which are related to glycolysis, were elevated in biofilms than planktonic cells (Fig. 5A). Metabolites involved in the pyruvate fermentation, such as lactate, pyruvate, malate, acetyl-coA, acetate, fumarate and succinate were increased in biofilms (Fig. 5B).

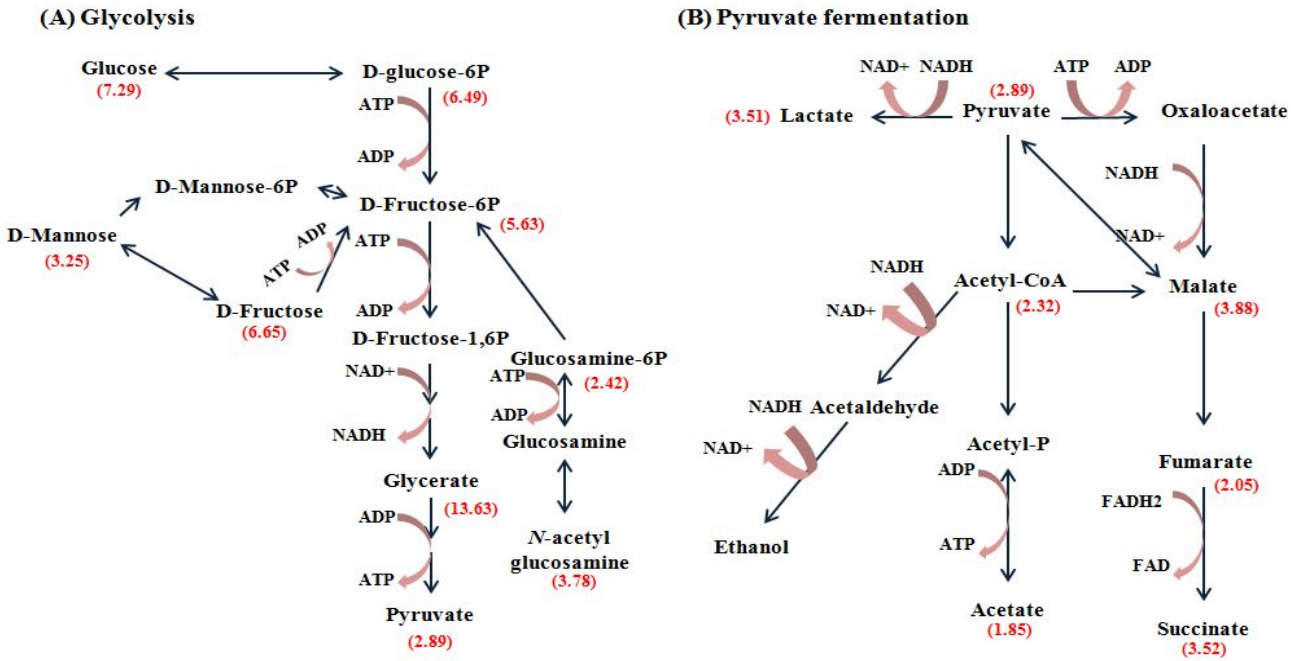

Fig. 5. Glycolysis (A) and Pyruvate Fermentation (B) in *V. vulnificus* MO6-24/O biofilms. The pathway was modified from the KEGG database. Red numbers indicate a fold change of metabolite in biofilms compared to planktonic cells in the metabolomic analysis.

Putrescine biosynthetic pathway analysis.

The polyamine putrescine is involved in modulating the synthesis of DNA, RNA, and protein (Igarashi & Kashiwagi, 2000; Tabor *et al.,* 1985; Yoshida *et al.,* 2004). Specific functions associated with the polyamine putrescine have been identified. For example, putrescine is a constituent of the outer membrane in some gram-negative bacteria (Koski & Vaara, 1991; Vinogradov & Perry, 2000) and putrescine have recently been shown to protect *E. coli* from toxic effects of oxygen (Chattopadhyay *et al*., 2003). Furthermore, putrescine has been shown to act as an extracellular signal required for swarming in *Proteus mirabilis* (Sturgill *et al*., 2004). Also, in *Yersinia pestis,* putrescine directly affects biofilm formation (Patel *et al.,* 2006).

As shown in Figure 6, the level of putrescine was greater in biofilms compared to the planktonic cells. And urea cycle related metabolites, including aspartate, citrulline and urea were smaller in biofilms, suggesting that urea cycle was inactivated, whereas putrescine biosynthetic pathway was activated in *V. vulnificus* biofilms. Therefore, putrescine may play an important role in formation of *V. vulnificus* biofilms.

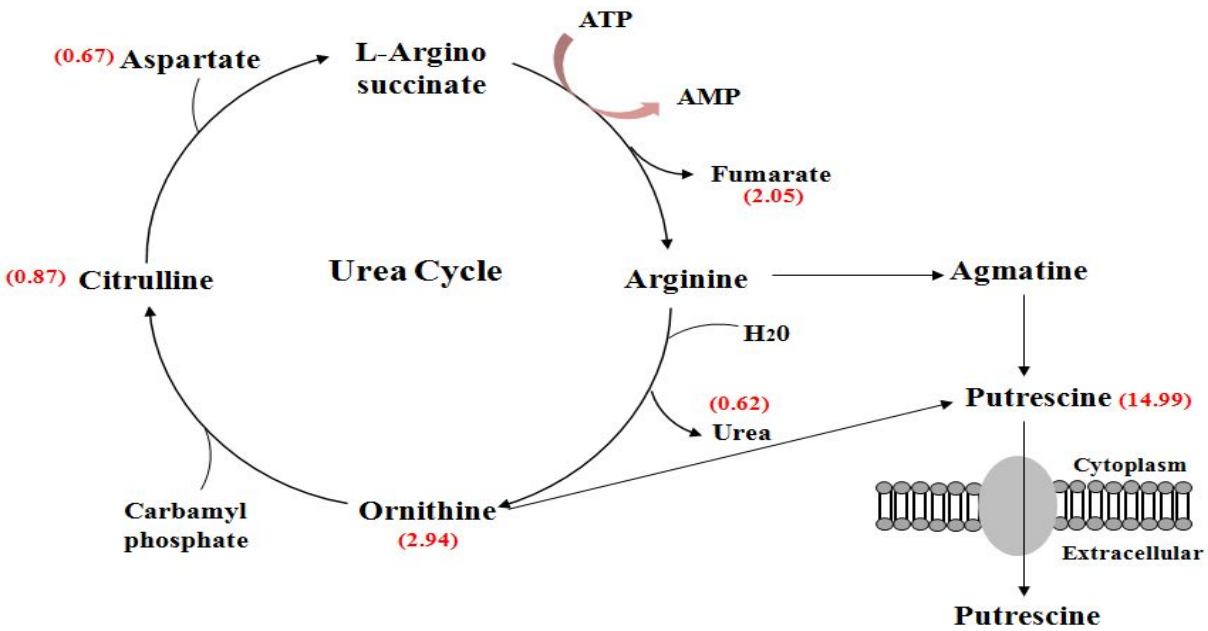

Fig. 6. Polyamine metabolism in *V. vulnificus* biofilms. The pathway was modified from the KEGG database. Red numbers indicate a fold change of metabolite in biofilms compared to planktonic cells in the metabolomic analysis.

_N_-acetylglucosamine, an important carbon source in _V. vulnificus_ biofilms.

_N_-acetylglucosamine (GlcNAc) appears to influence a variety of cellular processes, including energy metabolism, chitin utilization, competence, biofilm formation and pathogenicity in bacteria (Thompson *et al.,* 2011). The phosphotransferase system (PTS) has long been known to participate in regulation that impinges on metabolism, including chemotaxis, inducer exclusion and catabolite repression (Deutscher *et al.,* 2006). Furthermore, PTS pathways control biofilm formation by *V. cholerae* (Houot *et al.,* 2010).

As shown in Figure 7, in metabolomics analysis, GlcNAc utilization related metabolites, such as *N*-acetylglucosamine, *N*-acetylglucosamine-6-p, glucosamine-6-p, fructose-6-p and glucose-6-p were highly detected in biofilms. Also, in tanscriptomics analysis, the genes related with GlcNAc utilization, including *ptsG, nagA, nagB* and *pgi* gene were up-regulated, at least 2.01 fold to maximum 5.71 fold, in *V. vulnificus* biofilms (Park *et al*., unpublished) (Table 4). Consequently, the combined results suggest that, in mature biofilms, *V. vulnificus* tends to utilize GlcNAc.

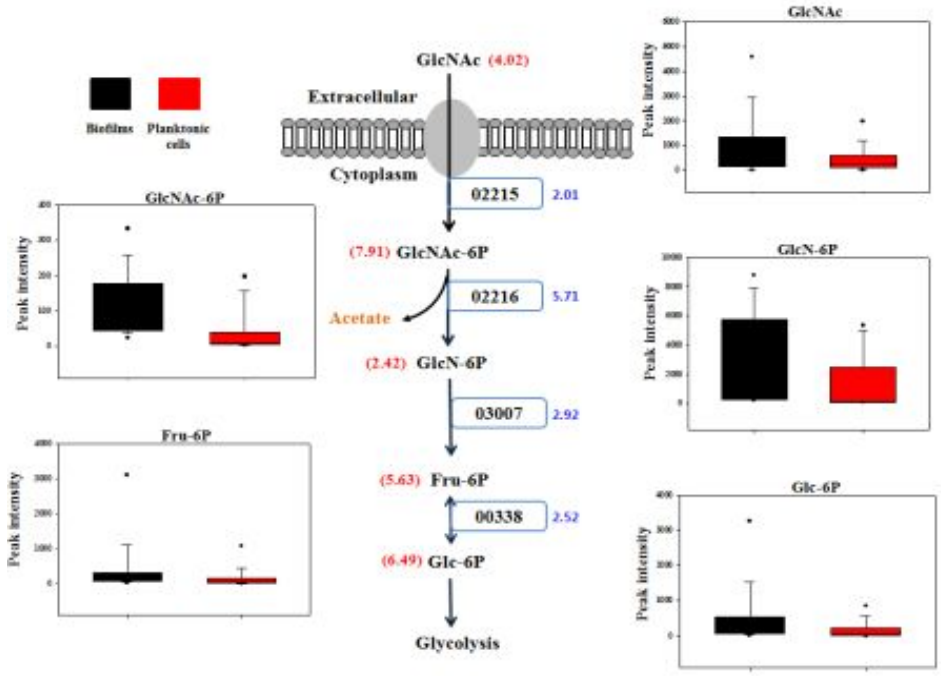

Fig. 7. *N*-acetylglucosamine(GlcNAc) specific phosphotransferase system(PTS) and GlcNAc utilization in *V. vulnificus* biofilms. The pathway was modified from the KEGG database. Red numbers indicate a fold change of metabolite in biofilms compared to planktonic cells in the metabolomic analysis. Blue numbers indicate a fold change of gene expression in biofilms compared to planktonic cells in the transcriptomic analysis (Park *et al*., unpublished). Box-whisker plots represent that GlcNAc, GlcNAc-6P, GlcN-6P, Fru-6P, and Glc-6P were highly detected in the *V. vulnificus* biofilms. GlcNAc, *N*-acetylglucosamine; GlcNAc-6P, *N*-acetylglucosamine-6-phosphate; GlcN-6P, Glucosamine-6-phosphate; Fru-6P, Fructose-6-phosphate; Glc-6P, Glucose-6-phosphate; black box; biofilms, red box; planktonic cells.

Table 4. Expression of GlcNAc-specific PTS genes in *V. vulnificus* biofilms revealed by RNA-seq analysis.

Locus tag	Gene	Function	Fold change	p-value	RPKM_ave
VVMO6_02215	***ptsG***	**Phosphotransferase system IIC components**	**2.0141**	**0.00856**	**241**
VVMO6_02216	***nagA***	***N*-acetylglucosamine-6-phosphate deacetylase**	**5.70814**	**0.00302**	**96.1**
VVMO6_03007	***nagB***	**Glucosamine-6-phosphate isomerase/deaminase**	**2.9197**	**0.00663**	**136.6**
VVMO6_00338	***pgi***	**Glucose-6-phosphate isomerase**	**2.51313**	**0.02766**	**581.5**

Composition analysis of wild type *V. vulnificus* EPS.

To confirm the hypothesis that constituent of *V. vulnificus* EPS, GlcNAc is liberated from biofilm matrix when the amount of biofilms reaches mature stage, EPS was extracted and composition analysis was conducted by GC-TOF-MS. All samples were prepared in biological duplicates and analytical duplicates.

The EPS of wild type *V. vulnificus* was composed of D-xylose, D-glucosamine, D-glucose, GlcNAc, ManNAc, L-arabinose, D-galactose, D-fructose and D-mannose in metabolomic analysis (Table 5).

Table 5. EPS composition of wild type *V. vulnificus* revealed by GC-TOF-MS analysis.

[a]Compound	[b]RT(min)	[c]MS Fragmentation(m/z)	[d]ID	[e]Peak Intensity
D-xylose	10.14	45,59,73,89,103,117,133,147,160,189,205,217 , 307	MS/STD	618.02
D-fructose	11.99	45,59,73,89,103,117,133,147,173,189,205,217, 277,307	MS/STD	424.92
D-galactose	12.16	45,59,73,89,103,117,129,147,160,189,205,217, 319	MS/STD	306.17
D-mannose	12.20	45,53,59,69,73,83,99,115,133,143,147,217,245	MS/STD	190.38
D-glucosamine	12.26	59,69,73,89,103,117,131,147,188,203,216,304	MS/STD	177.17
ManNAc	13.44	45,59,73,89,103,117,129,147,157,171,191,205, 217,229,319	MS/STD	115.75
D-glucose	12.18	59,73,103,147,189,205,319	MS/STD	104.42
L-arabinose	10.45	45,59,73,89,103,117,133,147,160,189,205,217, 307	MS/STD	92
GlcNAc	13.57	59,73,89,116,147,191,217,245	MS/STD	66.42

[a]Identified metabolites depended on variable importance projection (VIP) value under 0.7 and p-value <0.05.

[b]Retention time.

[c]m/z values are the selected ions for identification and quantification of individual derivatized metabolies.

[d]Identification: MS, mass spectrum was consistent with those of nist and in-house libraries; STD, mass spectrum was consistent with that of standard compound.

[e]Peak intensity: relative amount of metabolite.

Construction and confirmation of *V.vulnificus ptsG* mutant.

GlcNAc specific PTS IIC component, *ptsG* was selected for mutant target. To obtain insight into the role of *ptsG* on the molecular level, *V. vulnificus ptsG* mutant was constructed by allelic exchange (Fig. 8A). A double crossover, in which wild type *ptsG* gene was replaced with Δ *ptsG* allele, was confirmed by PCR using a pair of primers, PtsG_F1-F and PtsG_F2-R (Table 2). The PCR analysis of the genomic DNA from *V. vulnificus* MO6-24/O with the primers produced a 1.5-kb fragment, but the genomic DNA from Δ *ptsG* mutant resulted in an amplified DNA fragment approximately 0.7-kb in length (Fig. 8B).

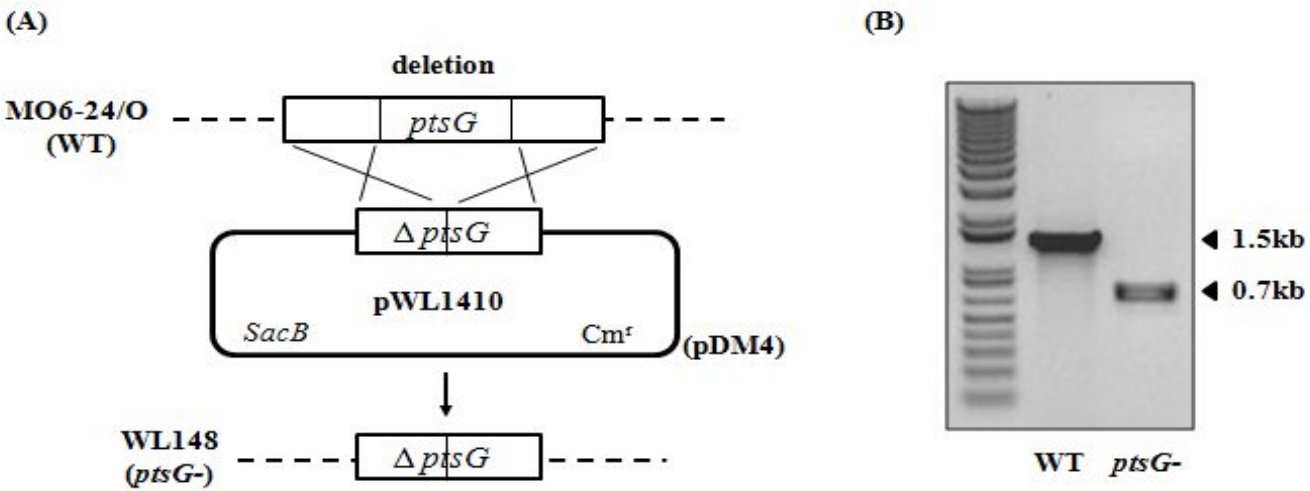

Fig. 8. Construction and confirmation of *V. vulnificus ptsG* mutant. (A) Homologous recombination between the chromosomal *ptsG* gene from wild type MO6-24/O and pWL1410 led to deletion of the *ptsG* gene and resulted in construction of the *ptsG* mutant. (B) The PCR analysis of the genomic DNA from *V. vulnificus* MO6-24/O and *ptsG* mutant produced a 1.5kb and 0.7kb fragments, respectively. sacB, levansucrase gene; Cm^r, chloramphenicol resistant.

Bofilm-forming activity of wild type and *ptsG mutan*t under various culture conditions.

To compare the biofilm forming ability of wild type and *ptsG* mutant, biofilm assay was conducted with modified VFMG. Carbon source (glycerol) in VFMG was modified in order to assess biofilm forming activity in low-nutrient environments. When the level of carbon concentration in VFMG was low, the *ptsG* mutant was reduced in biofilm forming activity compared to the wild type (Fig. 9A). Also, as shown in Figure 9B, biofilm forming ability was recovered in the complemented strain. These results showed that *ptsG* contributes to *V. vulnificus* biofilm formation.

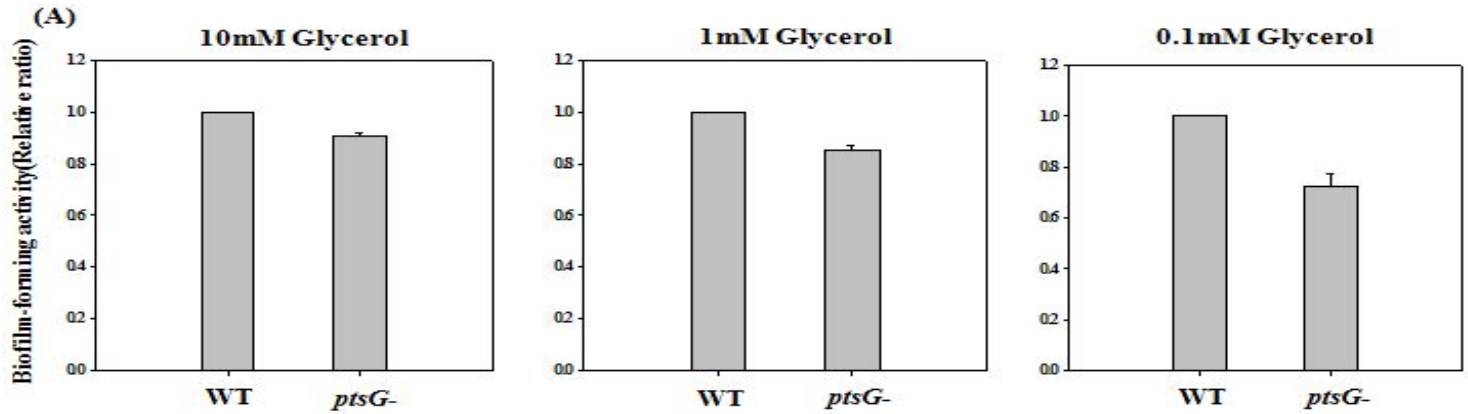

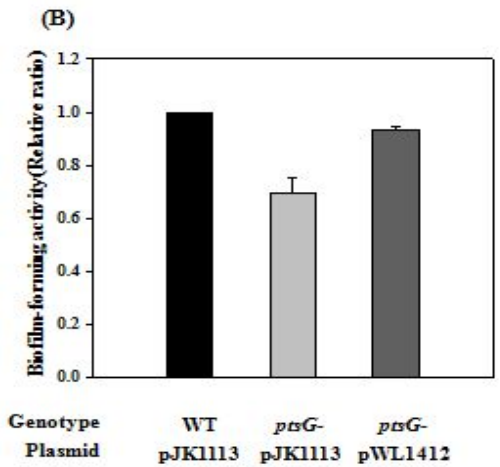

Fig. 9. Biofilm formation of wild type and *ptsG* mutant. (A) By using modified VFMG (containing 10, 1, 0.1mM glycerol), Biofilm assays were performed with crystal violet for quantifying biofilms. (B) Complementation. Abilities to form biofilms were determined using the crystal violet staining assay on cultures grown at 30℃ for 24 hours with 0.002% arabinose and 100 μg/ml kanamycin. WT (pJK1113), MO6-24/O; *ptsG*- (pJK1113), *ptsG* mutant; *ptsG*- (pWL1412), complemented strain.

IV. DISCUSSION

Microbes often construct and live within surface-associated multicellular communities known as biofilms. Biofilms are enclosed in a extracellular polymeric matrix that forms the scaffold for the three-dimensional architecture of the biofilms and is responsible for adhesion to surfaces and for cohesion in the biofilms (Flemming *et al.,* 2010). Also, biofilms contain bacterial cells that are in a wide range of physiological states. This heterogeneity is considered to be caused by gradients of pH, oxygen, and nutrients in the biofilm matrix (Stewart *et al.,* 2008). Given that these properties of biofilms have an impact on cellular metabolism, it can be expected that metabolism occurring in biofilms would be different from in planktonic cells.

In this study, in order to gain insight of into the cellular mechanisms of biofilms, I tried to conduct the global metabolite profiling of *V. vulnificus* biofilms and planktonic cells. The metabolome is much more sensitive to perturbations in the environment than either the transcriptome or the proteome because the metabolites within a cell are an integrated reflection of the cellular phenotype (Sellick *et al*., 2009). Therefore, metabolomics approach to understand the *V. vulnificus* biofilms is very significant.

There are three stages of biofilm development: (i) initial attachment, (ii) maturation,

(iii) dispersion. Here, to characterize mechanisms of mature biofilms, biofilms and planktonic cells were harvested at the peak time point (Fig. 1). Different from the other 'omics', metabolomics includes methodological problems derived from heterogeneity in chemical properties (Ohashi *et al*., 2008). In this reason, metabolome sampling is one of the most important factors determine the quality of metabolomics data (Kim *et al.,* 2013a). Thus, to minimize the losses of metabolites, I selected sample-dependent methods (Fig. 2).

From the experiment, principal component analysis and partial least-squares discriminant analysis revealed significant differences in metabolic profiles between biofilms and planktonic cells (Fig. 3). The levels of 37 metabolites, such as some amino acids, monosaccharides and nucleotides were elevated in biofilms compared to the planktonic counterparts (Table 3). EPM are mainly polysaccharides, proteins and nucleic acids (Flemming *et al.,* 2010). Therefore, most of these metabolites appear to function as building blocks for structural components of extracellular matrix.

Metabolites involved in the glycolysis and pyruvate fermentation were increased in biofilms (Fig. 5). These suggest that *V. vulnificus* may obtain energy by using glycolysis and pyruvate fermentation, when they are in biofilms. In a mature biofilms, at least three distinct physiological states can be anticipated (Stewart *et al.,* 2008). Especially, cells that are located deeper layer in the biofilms presumably grow by anaerobic metabolism. Therefore, to survive under unfavorable conditions,

cells in *V. vulnificus* biofilms may depend on glycolysis and pyruvate fermentation. In this manner, bacterial cells in *V. vulnificus* biofilms are possible for long-term survival.

In *V. vulnificus* biofilms, putrescine biosynthetic pathway related matabolites were greater than in the planktonic cells (Fig. 6). Urea cycle was inactivated, whereas putrescine biosynthetic pathway was activated in *V. vulnificus* biofilms. These results suggested that putrescine may have a positive effect on formation of *V. vulnificus* biofilms.

Bacteria seem to initiate biofilm development in response to specific environmental cues, such as nutrient availability. Then, these biofilms continue to develop as long as fresh nutrients are provided, but when they are nutrient deprived, they detach from the surface and return to a planktonic mode of growth (George *et al.,* 2000). In the experiment, the amounts and expression levels of the metabolites and genes, respectively, involved in *N*-acetylglucosamine (GlcNAc) utilization were highly increased in *V. vulnificus* biofilms. (Fig. 7). Composition analysis of EPS using GC-TOF-MS revealed that GlcNAc is one of the constituent of EPS (Table 5). Consequently, the combined results suggest that, in mature biofilms, when *V. vulnificus* exists in low-nutrient environments, GlcNAc specific PTS may transfer GlcNAc which is derived from EPS. Then, it may be possible to use the GlcNAc as a carbon source.

PTS consists of components of the carbohydrate-specific and PtsG is GlcNAc specific PTS IIC component (Houot *et al.,* 2010). In this study, to find out whether PtsG affects biofilm forming ability of *V. vulnificus,* I selected *ptsG,* for mutant target. Under the condition of low carbon source, biofilm forming activity was reduced in the *ptsG* mutant compared to the wild type and recovered in the complemented strain (Fig. 9). In these aspects, when bacterial cells in *V. vulnificus* biofilms are faced with adverse conditions, such as insufficient nutrient, PtsG transports GlcNAc which stems from EPS. Then, GlcNAc appears to be used as a carbon source.

Biofilms formed in industrial settings can be recalcitrant to antimicrobial agents, thereby leading to possible infection of food products (Kumar *et al.,* 1998). This study is expected to give important clues in understanding the cellular mechanisms of *V. vulnificus* biofilms. Also, in order to conduct more precise analysis of *V. vulnificus* biofilms, this study present combined other 'omics' study as an improved adaptation over prior microbial metabolomics studies. Through this study, it is revealed that some factors including biofilm-specific physiological pathways are important for *V. vulnificus* biofilm formation. If we use these factors in order to control biofilms, it can contribute to the food safety.

V. REFERNCES

A. Boyd & A.M. Chakrabarty. (1995). *Pseudomonas aeruginosa* biofilms: Role of the alginate exopolysaccharide. *Journal of industrial microbiology* **15**, 152–168.

Branda SS., Vik S., Friedman L. & Kolter R. (2005). Biofilms: The matrix revisited. *Trends in Microbiology* **13**, 20–26.

Chandra N. Patel, Brian W. Wortham, J. Louise Lines, Jacqueline D. Fetherston, Robert D. Perry & Marcos A. Oliveira. (2006). Polyamines Are Essential for the Formation of Plague Biofilm. *Journal of bacteriology* **7***, 2355-2363.*

Chattopadhyay, M. K., C. W. Tabor & H. Tabor. (2003). Polyamines protect *Escherichia coli* cells from the toxic effect of oxygen. *PNAS* **5**, 2261–2265.

Costerton JW. (2001). Cystic fibrosis pathogenesis and the role of biofilms in persistent infection. *Trends in Microbiology* **9**, 50-52.

Deutscher, J., C. Francke & P. W. Postma. (2006). How phosphotransferase system-related protein phosphorylation regulates carbohydrate metabolism in bacteria. *Microbiology and Molecilar Biology Reviews* **4**, 939–1031.

D.G. Davies, A.M. Chakrabarty & G.G. Geesey. (1993). Exopolysaccharide production in biofilms: Substratum activation of alginate gene expression by *Pseudomonas aeruginosa*. *Applied and Evironmental Microbiology* **4,** 1181–1186.

Enos-Berlage, J.L. & L.L. McCarter. (2000). Relation of capsular polysaccharide production and colonial cell organization to colony morphology in *Vibrio parahaemolyticus*. *Journal of bacteriology* **19,** 5513-20.

Fiehn, O. (2002). Metabolomics—The link between genotypes and phenotypes. *Plant molecular biology* **1_2**, 155–171.

Flemming, H.C., & W. Jost. (2010). The biofilm matrix. *Nature Reviews* **8,** 23-33.

George O'Toole, Heidi B. Kaplan & Roberto Kolter. (2000). Biofilm formation as microbial development. *Annual Review of Microbiology* **54,** 49-79.

Gwen Sturgill & Philip N. Rather. (2004). Evidence that putrescine acts as an extracellular signal required for swarming in *Proteus mirabilis. Molecular Microbiology* **2,** 437-446.

Hall-Stoodley L & Stoodley P. (2009). Evolving concepts in biofilm infections. *Cellular microbiology* **11,** 1034–1043.

Igarashi, K. & K. Kashiwagi. (2000). Polyamines: mysterious modulators of cellular functions. *Biochemical and biophysical research communications* **3,** 559–564.

Jones, M. K. & Oliver, J. D. (2009). *Vibrio vulnificus*: disease and pathogenesis. *Infection and Immunity* **77**, 1723–1733.

Kim, M., Park, J.M., Um, H.J., Lee K.H., Kim,H., Min, J. & Kim, Y., H. (2011). The antifouling potentiality of galactosamine characterized from *Vibrio vulnificus* exopolysaccharide. *Biofouling: The Journal of Bioadhesion and Biofilm Research* **8,** 851-857.

Kim, S., Lee, D. Y., Wohlgemuth, G., Park, H. S., Fiehn, O. & Kim, K. H. (2013a). Evaluation and optimization of metabolome sample preparation methods for *Saccharomyces cerevisiae*. *Analytical chemistry* **85**, 2169-2176.

Kim, S.M., Park, J.H., Lee, H.S., Kim, W.B., Ryu, H.J. & Choi, S.H. (2013). LuxR Homologue SmcR is Essential for *Vibrio vulnificus* Pathogenesis and Biofilm Detachment and Its Expression is Induced by Host Cells. *Infection and Immunity* **81**, 3721-3730.

Koski, P. & M. Vaara. (1991). Polyamines as constituents of the outer membranes of *Escherichia coli* and *Salmonella typhimurium*. *Journal of bacteriology* **12**, 3695–3699.

K. Sauer & A.K. Camper. (2001). Characterization of phenotypic changes in *Pseudomonas putida* in response to surface-associated growth. *Journal of bacteriology* **22,** 6579–6589.

Kumar CG& S.K Anand. (1998). Significance of microbial biofilms in food industry. *International Journal of Food Microbiology* **1-2,** 9-27.

Laetitia Houot, Sarah Chang, Bradley S. Pickering, Cedric Absalon & Paula I. Watnick. (2010). The Phosphoenolpyruvate Phosphotransferase System Regulates *Vibrio cholerae* Biofilm Formation through Multiple Independent Pathways. *Journal of bacteriology* **12**, 3055-3064.

Lin, C.Y. & Viant, M.R. (2006). Metabolomics: methodologies and applications in the environmental sciences. *Journal of Pesticide Science* **3**, 245–251.

Marcinowska, R., Trygg, J., Wolf-Watz, H., Mortiz, T. & Surowiec, I. (2011). Optimization of a sample preparation method for the metabolomic analysis of clinically relevant bacteria. *Journal of microbiological methods* **87**, 24-31.

Milton, D. L., R. O'Toole, P. Horstedt & H. Wolf-Watz. (1996). Flagellin A is essential for the virulence of *Vibrio anguillarum*. *Journal of bacteriology* **178,** 1310-1319.

M. Whiteley, M.G. Bangera, R.E. Bumgarner, M.R. Parsek, G.M. Teitzel, S. Lory & E.P. Greenberg. (2001). Gene expression in *Pseudomonas aeruginosa* biofilms, *Nature* **413,** 860–864.

Oh, M. H., S. M. Lee, D. H. Lee & S. H. Choi. (2009). Regulation of the *Vibrio vulnificus hupA* gene by temperature alteration and cyclic AMP receptor protein and evaluation of its role in virulence. *Infection and Immunity* **77,** 1208-1215.

Ohashi, Y., Hirayama, A., Ishikawa, T., Nakamura, S., Shimizu, K., Ueno, Y., Tomita, M. & Soga, T. (2008). Depiction of metabolome changes in histidine-starved *Escherichia coli* by CE-TOFMS. *Molecular BioSystems* **4**, 135-147.

P. Genevaux, S. Muller & P. Bauda. (1996). A rapid screening procedure to identify mini-Tn10 insertion mutants of *Escherichia coli* K-12 with altered adhesion properties. *FEMS microbiology letters* **1**, 27–30.

Philip S. Stewart & Michael J. Franklin. (2008). Physiological heterogeneity in biofilms. *Nature Reviews* **6,** 199-210.

P.N. Danese, L.A. Pratt & R. Kolter. **(2000).** Exopolysaccharide production is required for development of *Escherichia coli* K-12 biofilm architecture. *Journal of bacteriology* **12,** 3593–3956.

Sellick, C. A., Hansen, R., Maqsood, A. R., Dunn, W. B., Stephens, G. M., Goodacre, R. & Dickson, A. J. (2008). Effective quenching processes for physiologically valid metabolite profiling of suspension cultured mammalian cells. *Analytical chemistry* **81**, 174-183.

Shin, M. H., Lee, D. Y., Skogerson, K., Wohlgemuth, G., Choi, I. G., Fiehn, O. & Kim, K. H. (2010). Global metabolic profiling of plant cell wall polysaccharide degradation by *Saccharophagus degradans*. *Biotechnology and bioengineering* **105**, 477-488.

Shin, M. H., Lee, D. Y., Liu, K.-H., Fiehn, O. & Kim, K. H. (2010a). Evaluation of sampling and extraction methodologies for the global metabolic profiling of *Saccharophagus degradans*. *Analytical chemistry* **82**, 6660-6666.

Tabor, C. W. & H. Tabor. (1985). Polyamines in microorganisms. *Microbiological reviews* **1**, 81–99.

Thompson FL, Neto AA, Santos E de O, Izutsu K & Iida T. (2011). Effect of Nacetyl-D-glucosamine on gene expression in *Vibrio parahaemolyticus*. *Microbes*

and Environments **1,** 61–66.

Thompson FL, Neto AA, Santos E de O, Izutsu K & Iida T. (2011). Effect of Nacetyl-D-glucosamine on gene expression in *Vibrio parahaemolyticus*. *Microbes and Environments* **1,** 61–66.

Xianming Shi & Xinna Zhu. (2009). Biofilm formation and food safety in food industries. *Trends in Food Science & Technology* **9**, 407-413.

Yoshida, M., K. Kashiwagi, A. Shigemasa, S. Taniguchi, K. Yamamoto, H. Makinoshima, A. Ishihama & K. Igarashi. (2004). A unifying model for the role of polyamines in bacterial cell growth, the polyamine modulon. *Journal of Biological Chemistry* **47**, 46008–46013.

VI. 국문초록

Biofilm 은 extracellular polymeric matrix (EPM)이라는 미생물 스스로 만들어 낸 물질에 의해 둘러싸인 미생물 세포 군집이다. Biofilm 은 항생물질과 같은 여러 스트레스 조건하에서 미생물이 저항성을 가질 수 있도록 한다. 많은 병원성 박테리아처럼, 패혈증 비브리오균도 생물적 혹은 무생물적 환경에서 biofilm 을 만들 수 있다.

우선 패혈증 비브리오균에서 biofilm 이 형성되었을 때의 세포 내부 mechanism 을 알아보기 GC-TOF-MS 를 이용하여 mature 한 상태의 biofilm 과 planktonic cell 의 metabolome 을 분석해 보았다. 그 결과 패혈증 비브리오균의 biofilm 과 planktonic cell 은 metabolite 상 뚜렷한 차이가 있음을 확인하였다.

분석을 통해 패혈증 비브리오균의 biofilm 에서 여러 amino acid, monosaccharide, nucleotide 가 증가하는 것을 볼 수 있었다. 이는 패혈증 비브리오균 matrix 의 구성 성분을 이루는 것으로 예상된다. 또한 패혈증 비브리오균의 biofilm 에서 glycolysis, pyruvate fermentation 에 관련된 metabolite 들이 증가하였고 이는 biofilm 내에서 무산소적 에너지 생산이 이루어지는 것으로 보인다. 그리고 biofilm 에서 polyamine 생산 경로에 대한 metabolite 들도 증가하였는데, biofilm 의 형성에 중요한 역할을 하는 것으로 생각된다.

마지막으로 패혈증 비브리오균의 biofilm 에서 *N*-acetylglucosamine utilization 과 관련 metabolite 들과 *N*-acetylglucosamine specific PTS system (PtsG)과 하위의 해당 경로에 관련된 gene 또한 모두 증가하였다. 이를 토대로 패혈증 비브리오균이 탄소원이 부족해지는 상황에서 세포 외부로부터 PtsG 를 통해 *N*-acetylglucosamine 을 세포 안으로 이동시켜 탄소원으로 이용할 것이라는 추측을 하였다. 적은 탄소원 농도에서 *ptsG* mutant 는 wild type 보다 biofilm 형성이 억제되는 것을 볼 수 있었고, 이는 *ptsG* complementation 에 의해 회복되었다.

모든 결과를 종합해 보면, 패혈증 비브리오균의 biofilm 에서는 matrix 구성 성분의 합성, 무산소적 에너지 생산, polyamine metabolism, *N*-acetylglucosamine utilization 으로 대표되는 독특한 생장 양상을 보인다.

본 연구에서는 패혈증 비브리오균 biofilm 의 global metabolite profiling 을 수행하였고 biofilm formation 에 중요한 몇 가지 factor 를 밝혀내고자 하였다. 본 연구에서 밝혀진 factor 를 이용하여 biofilm 을 control 한다면 식품안전성 측면에 크게 기여할 수 있을 것이다.